Three-dimensional ultrasonic trapping of micro-particles in water with a simple and compact two-element transducer

A. Franklin, A. Marzo, R. Malkin, and B. W. Drinkwater

Citation: Appl. Phys. Lett. **111**, 094101 (2017);
View online: https://doi.org/10.1063/1.4992092
View Table of Contents: http://aip.scitation.org/toc/apl/111/9
Published by the American Institute of Physics

Three-dimensional ultrasonic trapping of micro-particles in water with a simple and compact two-element transducer

A. Franklin,[a] A. Marzo, R. Malkin, and B. W. Drinkwater
Faculty of Engineering, University of Bristol, Bristol BS8 1TR, United Kingdom

(Received 26 June 2017; accepted 16 August 2017; published online 28 August 2017)

We report a simple and compact piezoelectric transducer capable of stably trapping single and multiple micro-particles in water. A 3D-printed Fresnel lens is bonded to a two-element kerfless piezoceramic disk and actuated in a split-piston mode to produce an acoustic radiation force trap that is stable in three-dimensions. Polystyrene micro-particles in the Rayleigh regime (radius $\lambda/14$ to $\lambda/7$) are trapped at the focus of the lens (F# = 0.4) and manipulated in two-dimensions on an acoustically transparent membrane with a peak trap stiffness of 0.43 mN/m. Clusters of Rayleigh particles are also trapped and manipulated in three-dimensions, suspended in water against gravity. This transducer represents a significant simplification over previous acoustic devices used for micro-particle manipulation in liquids as it operates at relatively low frequency (688 kHz) and only requires a single electrical drive signal. This simplified device has potential for widespread use in applications such as micro-scale manufacturing and handling of cells or drug capsules in biomedical assays.
[http://dx.doi.org/10.1063/1.4992092]

Acoustic manipulation has found several applications in handling sensitive particles such as cells.[1] Various devices based on the controlled use of acoustic radiation force have been used to move,[2,3] sort,[4,5] combine,[6,7] and deform[8] micro-particles without any physical contact. In this regard, ultrasound offers a safer alternative to optical trapping with an applicability to a wider range of materials including larger particles and optically opaque substances.[9] In addition, for a given power input, the acoustic radiation force can be up to five orders of magnitude greater than that that can be achieved with light for macroscopic objects.[10,11]

Ultrasonic manipulation started with quasi one-dimensional (1D)[12] and two-dimensional (2D)[13] standing wave devices which trap Rayleigh particles (i.e., $a \ll \lambda$, where a is the particle radius and λ is the wavelength) in regular patterns. For example, 4-transducer devices have been used to trap micro-particles in regular grids for applications such as tissue engineering.[14–16] In these devices, the frequency or phase of the ultrasound sources is changed to produce simple movement of a particular distribution of particles.[17] More recently, array devices with transducers made of several small elements have been shown to trap and manipulate individual particles in the Rayleigh regime, for example, the individually addressable 64-element circular device in the study by Courtney *et al.*[2] achieved stable trapping and manipulation in 2D. Another approach for 2D trapping suggested by Lee[18,19] and Lam[20] is to operate outside of the Rayleigh regime. A focused beam generated by a single element can trap a particle in 2D in the Mie regime (i.e., particle diameter of the order of wavelength). However, the so-called microbeam devices require very high frequencies ($f > 100$ MHz), thus making them difficult to manufacture and necessitating expensive drive electronics. Phase encoded holograms[21] have been demonstrated for the 2D trapping of particles arranged in intricate patterns. However, the particles had to have negative acoustic contrast (lower density than the host fluid) which excludes several relevant particle-host combinations, such as cells in water or in any water-based biological media. Full 3D trapping has been recently realized by Marzo *et al.*[22] and Baresch *et al.*[10] using beam devices based on phased arrays, demonstrating the manipulation of Rayleigh particles in air and water, respectively. However, these beam devices require complex electronics and individually addressable array elements, hindering their wide scale applicability and potential in miniaturisation. Marzo *et al.*[23] showed that by carefully positioning the elements of an array, a small number of independent excitation signals are enough to produce stable 3D trapping of millimeter sized particles; however, this approach has only been validated in air.

The realization of an affordable and simple device for 3D trapping of microparticles in water (or similar medium) remains an open problem. Such a device would offer a viable technology for micro-scale manufacturing or bio-medical research, even when only single-sided access is available. Here, we use a two-element array transducer excited by a single electrical drive signal and demonstrate stable 3D trapping of positive acoustic contrast (higher density than the host fluid) particles in water. The transducer consists of a monolithic or *kerfless* two-element array excited in a split-piston mode so that the two halves of the disk vibrate out-of-phase with one another. The acoustic field emitted from this disk is then focused with a 3D-printed acoustic Fresnel lens bonded to its surface. As shown in Fig. 1(a), this results in a tweezer-like beam, termed a *twin-trap*,[22] which has a 3D acoustic potential-well at the focal point. The simplicity, micro-particle manipulation capability, and operation in water of the presented device enable potential applications in

[a]Author to whom correspondence should be addressed: a.franklin@bristol.ac.uk

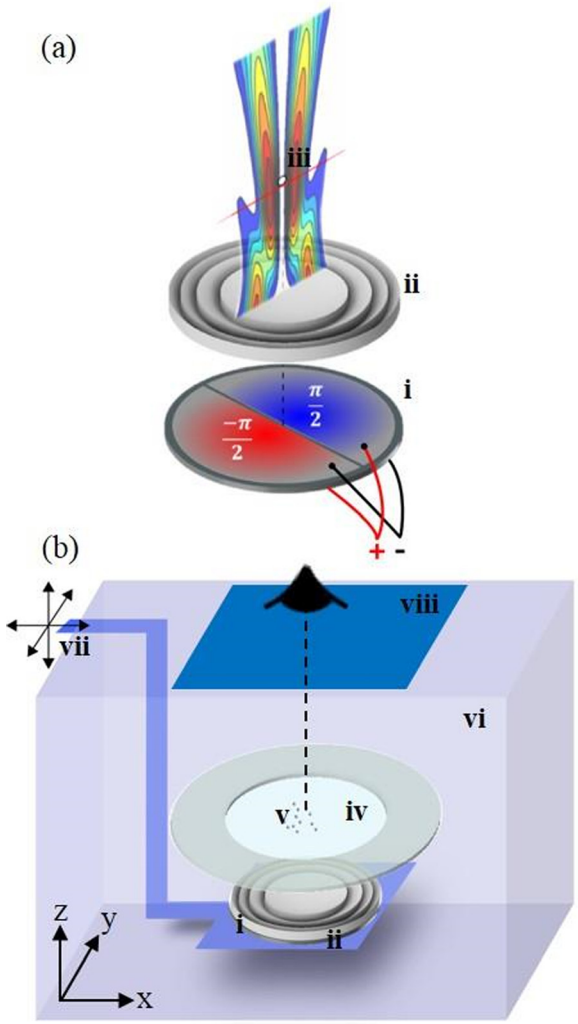

FIG. 1. (a) Exploded diagram of the transducer. (b) Schematic of the experimental set-up: (i) piezoceramic disk, (ii) Fresnel lens, (iii) particle trapped in the Twin-trap pressure field, (iv) acoustically transparent film, (v) microparticles, (vi) water tank, (vii) x-y-z stage, and (viii) absorbing material. The camera angle for Fig. 2 is shown.

biomedical assays such as cell-cell interaction studies[15] and targeted drug delivery.[24]

The schematic in Fig. 1(a) shows the transducer components: a piezoceramic disk patterned with two electrodes (each covering half of the disk), electric connections, and a bonded Fresnel acoustic lens. The piezoelectric disk (PZT-5H, Beijing Ultrasonic, P.R. China) has a diameter of 50 mm, a thickness of 3 mm, and silver wrap-around electrodes so that all the electrical connections are made on one side, permitting the other side to be bonded flat against the underside of the lens. As shown in Fig. 1(a), one half of the disk is wired with reversed polarity with respect to the other. This means that, when driven by a single electrical signal, the two halves are excited so that they vibrate out-of-phase with one another. The piezoelectric disk was bonded with an axis-symmetric Fresnel lens of 3.8 mm thickness (FLGPCL02 resin: speed of sound, $c = 2652$ m/s, density, $\rho = 1048$ kg/m^3, attenuation, $\alpha = 6.85$ dB/cm, and acoustic impedance, $Z_{SLA} = 2.78$ MRayl) that was 3D-printed using a Stereolithography Apparatus (SLA) printer (Form 2, Formlabs, MA, USA) with a print-layer thickness of 25 μm. The lens and the disk were bonded together using polyurethane glue (Waterproof Gorilla Glue, OH, USA). The lens profile was chosen to produce a focus at 20 mm from the surface ($f\# = 0.4$) using the geometric Fresnel lens design rules described by Mori *et al.*[25] Acoustic Fresnel lenses exploit the fact that the phase is cyclical (modulo 2π); for instance, in the frequency domain, a phase of 3π is the same as that of π. The thickness of the lens at each point is set to introduce a specific phase delay to create a focal point at the target. Since the phase is kept between 0 and 2π radians using the modulo operation, the lens acquires the characteristic shape of a Fresnel lens. In this way, a lens gets compressed into a thinner format, which results in lower attenuation compared to a regular lens and enables closer focusing. The piezoceramic disk and integrated lens were sealed around the exposed face with hot-melt adhesive to provide electrical insulation for the electrodes and to waterproof the device. In comparison to array devices, a tighter focus can be achieved with Fresnel lenses because the phase modulation is continuous and so each point of the surface contributes to the designed field shape.[21] However, the sound is attenuated by the lens, and the performance is dependent on the resolution and accuracy of the manufacturing technique, which in this case is an SLA 3D-printing. The lens material has an impedance reasonably well-matched to water ($Z_{water} = 1.52$ MRayl), resulting in efficient energy transfer from the lens into the fluid (i.e., a lens-water transmission coefficient of 0.914).

To select the optimal operating frequency for the transducer and to examine the performance of the kerfless array, the out-of-plane velocity amplitude of the piezo-electric disk was measured using a Laser Doppler Vibrometer (LDV) (Polytec PSV-400, Polytec GmbH, Waldbronn, Germany: sampling frequency = 2.56 MHz). Sweeping through frequencies close to the expected through-thickness resonance of the disk, a range of radial and flexural modes appear,[26] which allowed us to visualize the vibrational modes of the transducer (Fig. 2). The vibrometry analysis confirms that within a frequency band, the required out-of-phase actuation is achieved. We note that in general, kerfless arrays are not common as they are known to be susceptible to high cross-talk,[27] meaning that the relative phase of the elements is

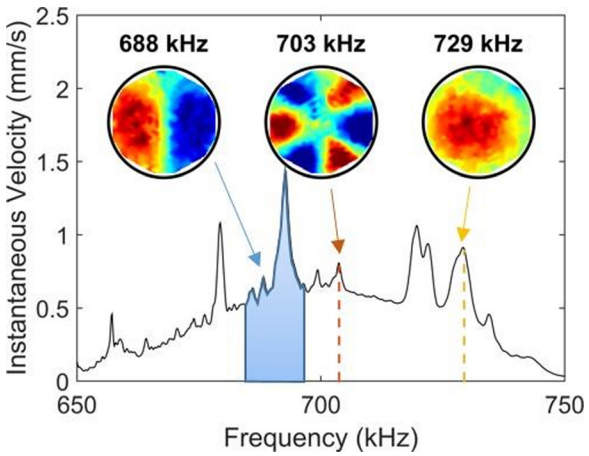

FIG. 2. Vibrometry data showing the average instantaneous velocity amplitude and vibration patterns of the transducer around the through thickness resonance.

hard to control individually. However, in this application, they are suitable because only a simple surface velocity pattern is required and the relative phase of the two elements does not need further control. The frequency range for the out-of-phase vibrational mode for this disk was found to be 686–696 kHz, shown as the blue shaded band in Fig. 2. We note that the resonance of the disk with the bonded lens was 2.5 kHz lower than that of the lens alone which was assumed to be small enough that high amplitude vibration of the device would still be achieved at the frequencies found from the vibrometry analysis.

The transducer was driven with a 688 kHz continuous sine wave created by a signal generator (33220A, Agilent Technologies, USA) and connected to a linear amplifier (75A250A, Amplifier Research, USA). We note that in water, this corresponds to a wavelength of $\lambda = 2.10$ mm; this wavelength sets the scale of the particles that can be manipulated. As our device operates in the Rayleigh regime, it is in principle suitable for particles in the range of $a = 21$ to 210 μm (i.e., $\lambda/100 - \lambda/10$).[28] The assembled transducer was then attached to a submerged platform that could be moved and repositioned in 3D with a mechanical x-y-z stage. A fixed sheet of acoustically transparent Low-Density Polyethylene (LDPE) film (thickness = 19 μm) was placed horizontally above the transducer to serve as a resting surface for the particles. An absorbing layer (Aptflex F28, Pressure Acoustics, UK; 10 mm in thickness, $Z_{F28} = 1.5$ MRayl) was positioned at the surface of the water to reduce reflections that could generate unwanted standing waves. The transducer could be raised or lowered so that the focal point was in the same plane as the LDPE film, allowing particles resting on the film to be held in the *twin-trap*. The particles were spherical polystyrene beads ($\rho = 1055$ kg/m^3 and c = 2350 m/s) with radii ranging from $a = 150$ to 300 μm. To capture the manipulation of the particles, a camera (D610, Nikon, Japan) with a macrolens (105 mm F2.8 EX DG Macro HSM, Sigma Imaging, UK) was positioned outside of the tank pointing towards the LDPE film from above.

2D manipulation of polystyrene micro-particles across the surface of the LPDE film (i.e., x- and y-direction) is shown in Fig. 3. In these experiments, the transducer was driven at 45 V_{pp} and the positioning stage was operated manually at a rate of approximately 5 mm/s. The particles can be seen to follow the location of the acoustic trap and can be manipulated to any location on the LPDE film (i.e., within a 50 mm radius circle). Figures 3(a) and 3(b) show that particles of different sizes can be trapped, from a radius of $\lambda/14$ to $\lambda/7$. Fig. 3(c) shows that clusters or lines of small particles can be trapped. We observed that the trapped particle clusters tended to form into agglomerates of a shape that matched that of the predicted trapping field (see the first row of Fig. 3), proving that the particles were trapped by a *twin-trap* and not by a parasitic standing wave.

3D manipulation of particles is presented in Fig. 4. We note that to achieve stable 3D trapping, the drive voltage was increased to 75 V_{pp}. First, the focal point was positioned just above the film to lift particles from the film surface and suspend them in the water, with the acoustic radiation force counteracting gravity. Then, the trapped particles were translated horizontally outside of the film where the particles were moved both vertically (z-direction) and horizontally (x-direction).

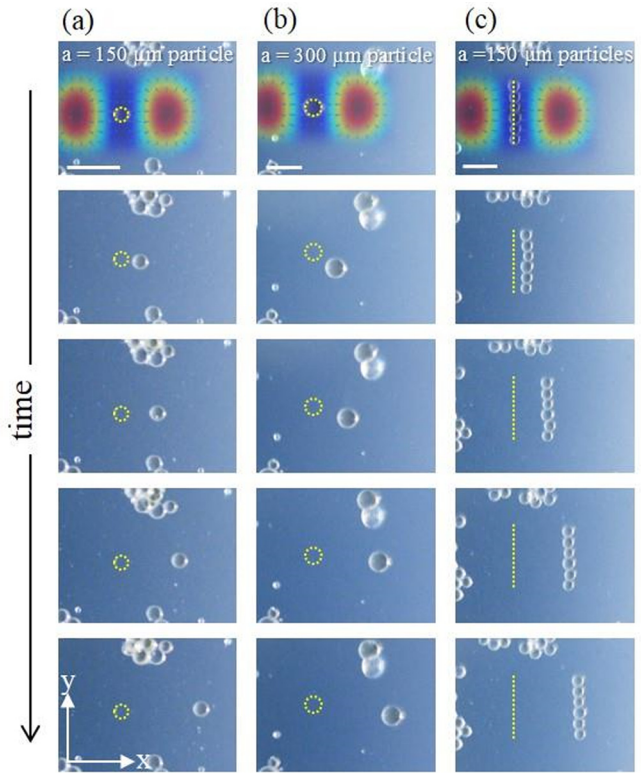

FIG. 3. Photographs of particles being manipulated; (a) 150 μm, (b) 300 μm, and (c) a cluster of six 150 μm radius polystyrene micro-beads. The dashed shapes show the starting position of each set of particles. The top row also shows the simulated acoustic potential field in the plane of the manipulation. All scale bars are 1 mm.

The Gor'kov potential was simulated using a semi-analytical Huygens model where the lens surface was discretised into monopole sources (using 20 point sources per λ_{water}) and the total pressure field was calculated from the

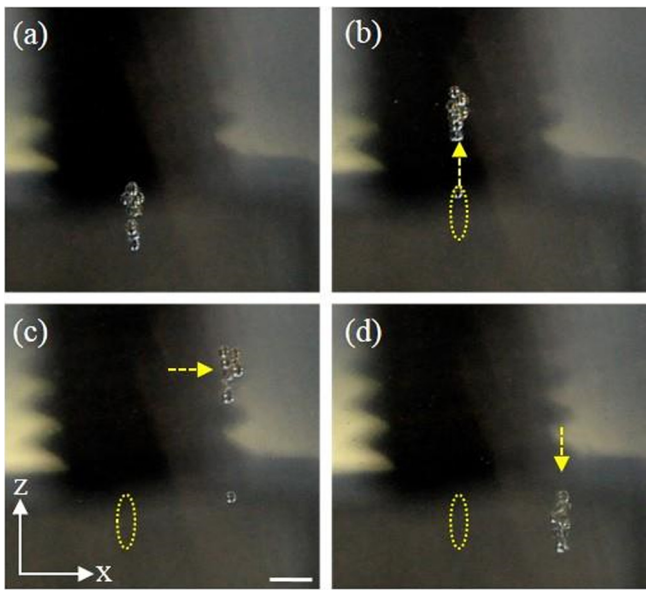

FIG. 4. Photographs of a cluster of 150 μm particles trapped and manipulated in 3D. The dashed ellipse indicates the starting point of the cluster, and the arrows indicate the path of the particles between frames, with time increasing from (a) to (d). The scale bar is 1 mm.

sum of the contributions from these monopoles. From this pressure field, the acoustic radiation potential on the polystyrene particles was calculated.[29] Figures 5(a) and 5(b) present the simulated normalised Gor'kov potential landscape in the xy-plane and xz-plane, respectively, showing the characteristic shape of the *twin-trap*. Figures 5(c)–5(e) show the acoustic radiation force (calculated as the negative gradient of the potential) acting on the particle in each direction through the focal point, demonstrating that the trap is a 3D potential well.

The trapping force and stiffness at the trap centre were inferred from the dynamic behaviour of particles moving from positions of high Gor'kov potential to the equilibrium position of the trap.[10] To record the behaviour of particles in the *twin-trap*, they were filmed at 1000 fps with a high-speed camera (Photron SA1, Photron, USA) recording perpendicular to the particle motion. An $a = 150\,\mu$m particle was positioned at $x = 0.3$ mm (where the origin is the trap centre), whilst the device was switched off. Then, the device was switched on (voltage $= 45\ V_{pp}$), and the particle motion in the x-direction was recorded. The particles took $\approx$40 ms to move to the equilibrium position (maximum measured velocity, $v_{max} = 13.8$ mm/s). The particle trajectories (average of 5 taken) were used to calculate particle velocity as a function of space and time. The acoustic trapping force can then be estimated by assuming a simple balance,[10] $m_p \frac{dv(x)}{dt} = F_s + F_{AM} + F_x$, where m_p is the mass of the particle, $v(x)$ is the velocity in the x-direction, $F_s = 6\pi\mu a v(x)(1 + 0.15\mathrm{Re}^{0.687})$ is the Stokes Drag, $F_{AM} = \frac{2}{3}\pi a^3 \rho_f \frac{dv(x)}{dt}$ is the added mass force due to the acceleration of the displaced fluid, and F_x is the acoustic radiation force in the x-direction. Note that here we cannot make the common microfluidic assumption and neglect inertia[30] as the particle Reynolds number $\mathrm{Re} > 1$.[31] Thus, the measured velocity and acceleration of the microparticle were used to estimate F_x on the particles. The stiffness of the trap (k_x) was calculated as the gradient of the force, $F_x = -k_x x$, and had a maximum at the trap centre of $k_x = 0.43$ mN/m. In the vicinity of the trap, the stiffness remains close to this maximum value, falling by 10% at a distance of 100 μm from the trap centre. The maximum measured force was 0.10 μN at a distance of 240 μm from the trap centre although we note that the force calculation does not consider the Basset force or the effect of the film boundary under the particle. From the Gor'kov model, the maximum forces in the y- and z-directions are found to be $\max(F_x)/83.3$ and $\max(F_x)/253.8$, respectively.

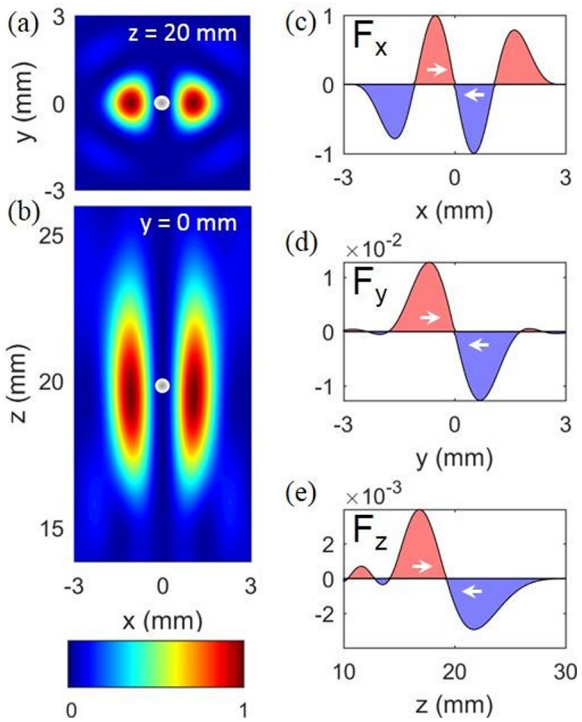

FIG. 5. Normalised acoustic radiation potential: (a) xy-plane and (b) xz-plane. The trap position is shown by the white circle. Acoustic radiation force: (c) x-axis, (d) y-axis, and (e) z-axis. All the forces have been normalized to F_x, where the maximum $F_x = 1$.

We have demonstrated a simple and compact transducer capable of generating stable 3D acoustic traps that can hold particles against gravity and translate them through water. This transducer was made of a kerfless array combined with an integrated 3D-printed Fresnel lens. Its reduced complexity and the requirement of only one driving signal represent a significant simplification over previous particle manipulation systems. This device will facilitate new potential research and applications such as the transport of micro-particles for contactless production processes, bio-medical assays, or targeted drug delivery.

A.F. was funded through an EPSRC DTP studentship. A.M. and R.M. were funded by the UK Engineering and Physical Science Research Council (EP/N014197/1) and (EP/N017641/1). All the data needed to reproduce the results are contained in this paper.

[1]M. Antfolk, C. Magnusson, P. Augustsson, H. Lilja, and T. Laurell, Anal. Chem. **87**, 9322–9328 (2015).
[2]C. R. P. Courtney, C. E. M. Demore, H. Wu, A. Grinenko, P. D. Wilcox, S. Cochran, and B. W. Drinkwater, Appl. Phys. Lett. **104**, 154103 (2014).
[3]T. Laurell, F. Petersson, and A. Nilsson, Chem. Soc. Rev. **36**, 492 (2007).
[4]P. Augustsson, J. T. Karlsen, H.-W. Su, H. Bruus, and J. Voldman, Nat. Commun. **7**, 11556 (2016).
[5]C. Devendran, I. Gralinski, and A. Neild, Microfluid. Nanofluid. **17**, 879–890 (2014).
[6]D. Foresti, M. Nabavi, M. Klingauf, A. Ferrari, and D. Poulikakos, Proc. Natl. Acad. Sci. **110**, 12549-12554 (2013).
[7]M. Caleap and B. W. Drinkwater, Proc. Natl. Acad. Sci. U. S. A. **111**, 6226 (2014).
[8]P. Mishra, M. Hill, and P. Glynne-Jones, Biomicrofluidics **8**, 034109 (2014).
[9]M. A. B. Andrade, A. L. Bernassau, and J. C. Adamowski, Appl. Phys. Lett. **109**, 044101 (2016).
[10]D. Baresch, J.-L. Thomas, and R. Marchiano, Phys. Rev. Lett. **116**, 024301 (2016).
[11]A. Jannasch, A. F. Demirörs, P. D. J. van Oostrum, A. van Blaaderen, and E. Schäffer, Nat. Photonics **6**, 469 (2012).
[12]A. Haake and J. Dual, J. Acoust. Soc. Am. **117**, 2752 (2005).
[13]S. B. Q. Tran, P. Marmottant, and P. Thibault, Appl. Phys. Lett. **101**, 114103 (2012).
[14]Y. Zhou Yufeng, Molecules **21**, 590 (2016).
[15]F. Guo, P. Li, J. B. French, Z. Mao, H. Zhao, S. Li, N. Nama, J. R. Fick, S. J. Benkovic, and T. J. Huang, Proc. Natl. Acad. Sci. U. S. A. **112**, 43 (2015).
[16]F. Gesellchen, A. L. Bernassau, T. Déjardin, D. R. S. Cumming, and M. O. Riehle, Lab Chip **14**, 2266 (2014).
[17]P. Glynne-Jones, R. J. Boltryk, and M. Hill, Lab Chip **12**, 1417 (2012).
[18]J. Lee, S.-Y. Teh, A. Lee, H. H. Kim, C. Lee, and K. K. Shung, Appl. Phys. Lett. **95**, 073701 (2009).
[19]Y. Li, C. Lee, R. Chen, Q. Zhou, and K. K. Shung, Appl. Phys. Lett. **105**, 173701 (2014).

[20]K. H. Lam, H.-S. Hsu, Y. Li, C. Lee, A. Lin, Q. Zhou, E. S. Kim, and K. K. Shung, Biotechnol. Bioeng. **110**, 881 (2013).
[21]K. Melde, A. G. Mark, T. Qiu, and P. Fischer, Nature **537**, 518 (2016).
[22]A. Marzo, S. A. Seah, B. W. Drinkwater, D. R. Sahoo, B. Long, and S. Subramanian, Nat. Commun. **6**, 8661 (2015).
[23]A. Marzo, A. Ghobrial, L. Cox, M. Caleap, A. Croxford, and B. W. Drinkwater, Appl. Phys. Lett. **110**, 014102 (2017).
[24]K. Kooiman, H. J. Vos, M. Versluis, and N. De Jong, Adv. Drug Delivery Rev. **72**, 28 (2014).
[25]K. Mori, A. Miyazaki, H. Ogasawara, T. Nakamura, and Y. Takeuchi, Jpn. J. Appl. Phys., Part 1 **46**, 4990 (2007).
[26]N. Guo, P. Cawley, and D. Hitchings, J. Sound Vib. **159**, 115 (1992).
[27]C. E. M. Demore, J. A. Brown, and G. R. Lockwood, IEEE Trans. Ultrason. Ferroelectr. Freq. Control **53**, 1046 (2006).
[28]B. W. Drinkwater, Lab Chip **16**, 2360 (2016).
[29]L. P. Gor'kov and L. P., Sov. Phys. Dokl. **6**, 773 (1962).
[30]H. Bruus, Lab Chip **12**, 1014 (2012).
[31]Z.-G. Feng and J. Dispers, Sci. Technol. **31**, 968–974 (2010).